



Perspectives on the Growth of High Edge Density Carbon Nanostructures: Transitions from Vertically Oriented Graphene Nanosheets to Graphenated Carbon Nanotubes

Stephen M. Ubnoske

Department of Mechanical Engineering and Materials Science, Pratt School of Engineering, Duke University, Durham, North Carolina 27708, United States

Akshay S. Raut, Billyde Brown, and Charles B. Parker*

Department of Electrical and Computer Engineering, Pratt School of Engineering, Duke University, Durham, North Carolina 27708, United States

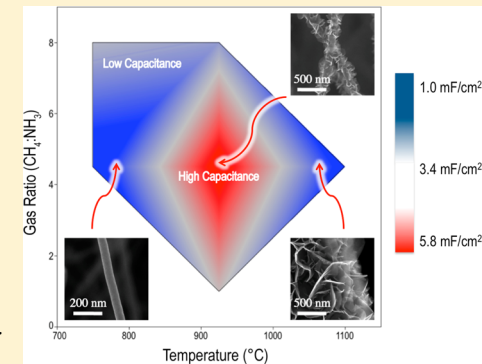
Brian R. Stoner

Discovery-Science-Technology Division, RTI International, Durham, North Carolina 27709, United States

Jeffrey T. Glass

Department of Electrical and Computer Engineering, Pratt School of Engineering, Duke University, Durham, North Carolina 27708, United States

ABSTRACT: Insights into the growth of high edge density carbon nanostructures were achieved by a systematic parametric study of plasma-enhanced chemical vapor deposition (PECVD). Such structures are important for electrode performance in a variety of applications such as supercapacitors, neural stimulation, and electrocatalysis. A morphological trend was observed as a function of temperature whereby graphenated carbon nanotubes (g-CNTs) emerged as an intermediate structure between carbon nanotubes (CNTs) at lower temperatures and vertically oriented carbon nanosheets (CNS), composed of few-layered graphene, at higher temperatures. This is the first time that three distinct morphologies and dimensionalities of carbon nanostructures (i.e., 1D CNTs, 2D CNSs, and 3D g-CNTs) have been synthesized in the same reaction chamber by varying only a single parameter (temperature). A design of experiments (DOE) approach was utilized to understand the range of growth permitted in a microwave PECVD reactor, with a focus on identifying graphenated carbon nanotube growth within the process space. Factors studied in the experimental design included temperature, gas ratio, catalyst thickness, pretreatment time, and deposition time. This procedure facilitates predicting and modeling high edge density carbon nanostructure characteristics under a complete range of growth conditions that yields various morphologies of nanoscale carbon. Aside from the morphological trends influenced by temperature, a relationship between deposition temperature and specific capacitance emerged from the DOE study. Transmission electron microscopy was also used to understand the morphology and microstructure of the various high edge density structures. From these results, a new graphene foliate formation mechanism is proposed for synthesis of g-CNTs in a single deposition process.



INTRODUCTION

Nanostructured carbon materials have existed as a prominent area of materials research for over two decades, from the discovery of Buckminsterfullerenes¹ to carbon nanotubes² and more recently graphene,³ including freestanding carbon nanosheets⁴ with thickness less than 1 nm. Recent reviews of graphene synthesis can be found in refs 5–7. Combinations of CNT and graphene materials systems have been reported in

two-stage processes^{8–10} using plasma-enhanced chemical vapor deposition (PECVD), and intrinsic chemical bonding between few-layered graphene (FLG) sheets and the carbon nanotube (CNT) framework was demonstrated.⁹ Potential applications

Received: March 6, 2014

Revised: June 9, 2014

Published: June 26, 2014



of these graphene/CNT hybrid materials include supercapacitors,^{11,12} lithium ion batteries,¹³ transparent conductive electrodes,¹⁴ neural stimulation electrodes,¹⁵ and carbon nanotube field effect transistors.¹⁶

Recently, we have developed a single PECVD process^{15,17} to grow few-layered graphene on the sidewalls of carbon nanotubes, referred to as graphenated carbon nanotubes (g-CNTs) (Figure 1). The current contribution further develops

our understanding of the nature of this simultaneous CNT/FLG hybrid growth and the growth of related high edge density carbon nanostructures. The importance of deposition temperature on carbon nanostructure morphology and dimensionality is highlighted. Additionally, a connection between deposition temperature, graphene edge density, and specific capacitance is provided, and an alternative phenomenological growth model is proposed.

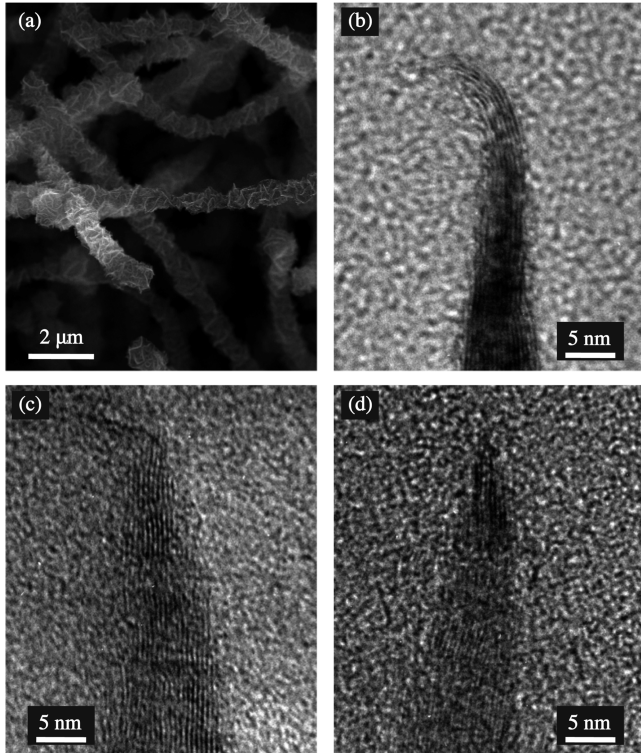


Figure 1. (a) Scanning electron microscopy (SEM) and (b–d) high-resolution transmission electron microscopy (HR-TEM) micrographs of the graphenated carbon nanotube structure. The FLG “foliates” reduce to approximately 3–5 graphene layers at the edge.

EXPERIMENTAL SECTION

Carbon Nanostructure Preparation. N-type conductive silicon (100) wafers with resistivity of $1 \Omega/\text{cm}$ were coated with iron catalyst at RTI International using a CHA electron beam evaporation system. Wafers were coated with 2, 5, or 12 nm Fe catalyst layers, yielding three different thicknesses for the parametric study.

Carbon nanostructures were grown using a 915 MHz microwave plasma-enhanced chemical vapor deposition (MPECVD) system. Substrates initially undergo a temperature ramp-up step during which the substrate is raised to the desired deposition temperature in 100 sccm NH_3 , followed by striking and tuning a plasma at 21 Torr and 2.1 kW of magnetron input power. The process then enters the pretreatment phase, and the process parameters remain constant as the iron film dewets into catalyst nanoparticles. The deposition phase begins by changing the gas flow to the desired ratio of $\text{CH}_4:\text{NH}_3$. Details of the deposition system can be found in Cui et al.¹⁸

Prior to each deposition experiment, substrates were cleaned in acetone and isopropanol. Repeatability was ensured by cleaning the deposition chamber with isopropanol between each experiment and performing a growth cycle without a substrate present to season the chamber. The purpose of this preliminary growth cycle was to bring the chamber to a reproducible state by exposure to a known amount of carbon prior to sample deposition on a substrate. During these seasoning runs, the chamber was heated to 850°C in 100 sccm NH_3 . Pretreatment continued for 15 min in NH_3 plasma, and deposition proceeded for 15 min using a gas flow of 150 sccm CH_4 and 50 sccm NH_3 .

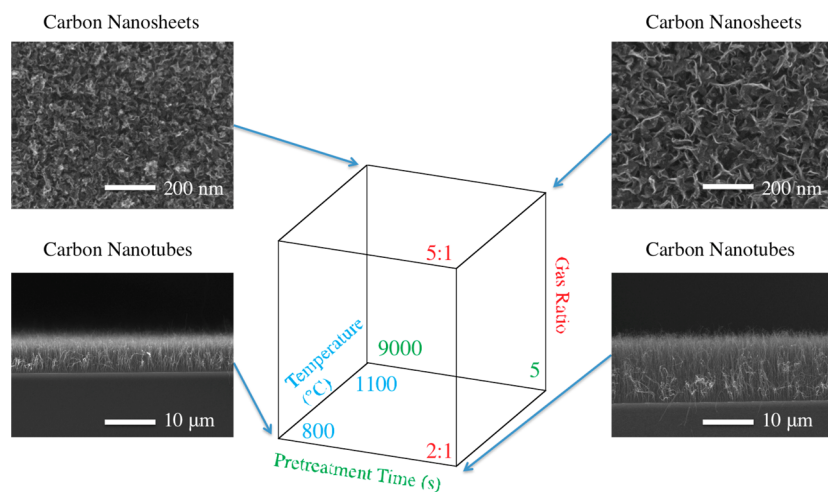


Figure 2. Factors affecting carbon nanostructure morphology. A set of DOE screening experiments preceded the full process space analysis for the purpose of identifying key factors that most strongly affect carbon nanostructure morphology. The screening runs, in this case, highlight the temperature-driven shift from the CNT to CNS morphology. Both of the pictured experiments performed at 1100°C and a 5:1 $\text{CH}_4:\text{NH}_3$ ratio resulted in the CNS morphology, while both films grown at 800°C and 2:1 $\text{CH}_4:\text{NH}_3$ ratio were carbon nanotubes.

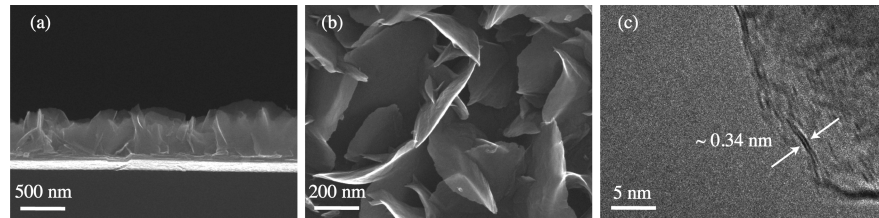


Figure 3. (a) Cross-sectional SEM image of carbon nanosheets grown at conditions similar to those obtained in the DOE screening experiments. (b) Top-view SEM image of typical carbon nanosheets. (c) HR-TEM micrograph of a single nanosheet with two graphene layers, as seen by the two parallel fringes.

The screening experiments preceding the DOE employed a process space, as seen in Figure 2, composed of temperature, pretreatment time, and gas ratio. Probing the corners of this cube revealed vertically aligned CNTs on the 800 °C plane and ribbonlike carbon nanosheets on the 1100 °C face (Figure 2). All screening runs used 5 nm Fe catalyst thickness and 120 s deposition time. The temperature, pretreatment time, and gas ratio for the various structures can be found in Figure 2. The carbon nanosheet morphology has been described previously as ultrathin sheet-like carbon nanostructures composed of vertical graphene layers.¹⁹ This nanosheet morphology was achieved using the same substrate and growth conditions, aside from temperature, as those used for carbon nanotube films (Figure 3). The full experimental design incorporated temperature, gas ratio, pretreatment time, deposition time, and catalyst thickness as factors and capacitance, Raman D/G ratio, CNT diameter, presence of CNTs, presence of CNSs, and second-order Raman scattering from Si as responses. While some of these results are outside the scope of this report, the effect of temperature on the DOE responses of greatest interest for high edge density carbon nanostructures are reported, including capacitance, presence of CNTs, and presence of CNSs.

Electrochemical Measurements. The electrochemical setup, including the cell and sample preparation, have been discussed in detail in a previous publication.²⁰ Briefly, a three-terminal electrochemical cell with working, counter, and reference electrodes (K0235 by Princeton Applied Research) was used. The working electrode was the nanostructured electrode under study, the counter electrode a Pt mesh (3–2.5 cm), and the reference a Ag wire in 1 M tetrabutylammonium perchlorate (TBAP) and 0.01 M silver nitrate (AgNO_3) in acetonitrile (reference electrode RE-7 and its solution supplied by BioLogic). The reference electrode resided in a separate subsection of the cell connected to the region near the double-layer interface of the working electrode by a Luggin–Haber capillary tube. The electrolyte used was 1 M LiClO_4 in acetonitrile. The potentiostat was a Bio-Logic SP-300. All chemicals were used as received.

For the electrochemical measurements, the sample was mounted on a piece of sheet metal using copper tape. An electrical contact was made by painting conductive silver epoxy on the nanostructure side. The nominal active area of the electrode as defined by a polytetrafluoroethylene gasket was 1.43 mm^2 .

Area specific capacitance was calculated using cyclic voltammetry for scans taken at a scan rate of 100 mV/s for each sample. Specific capacitance was calculated using the expression²¹

$$C \left[\frac{\text{F}}{\text{cm}^2} \right] = \frac{\int_{V_1}^{V_2} i(E) \, dE}{\nu(V_2 - V_1)A}$$

where C is the area specific capacitance and $i(E)$ is the instantaneous current (A); V_1 and V_2 are the voltage end points (V); ν is the scan rate (V/s), and A is the nominal area of the sample (cm^2). Finally, the integral term in the numerator is the total voltammetric charge obtained in the positive sweep of the voltage in the window ($V_2 - V_1$).

RESULTS AND DISCUSSION

Temperature Effects on Morphology. The most influential factor in determining film morphology during the parametric study was temperature (Figure 4). By varying

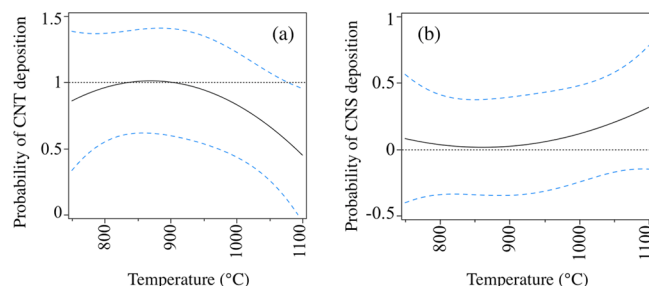


Figure 4. Standard least-squares prediction profiles illustrating relative likelihood of achieving (a) CNT or (b) CNS morphology based on varying temperature. The least-squares curves were obtained from data gathered during the design of experiments parametric study. The dashed curves, including the curve below zero, depict the 95% confidence intervals.

temperature alone, the resultant film could consist of carbon nanotubes, graphenated carbon nanotubes, or carbon nanosheets. The deposition probabilities in Figure 4 are defined as the number of experiments performed that resulted in the given structure divided by the total number of experiments performed at that temperature. The solid curve is a standard least-squares regression profile based on experimental data from all run conditions used in the DOE study. To further illustrate this result, a temperature series from 950 to 1150 °C was conducted using growth conditions of 180 s pretreatment time, 120 s deposition time, 5:1 $\text{CH}_4:\text{NH}_3$ ratio, and 5 nm Fe catalyst layer for each experiment. As seen in Figure 5, an increase in process temperature from 950 to 1000 °C transitions the resultant nanostructures from CNTs to g-CNTs. When the growth temperature reaches 1100 °C, the film is composed of CNSs with no nanotubes present. Thus, g-CNTs have emerged as an intermediate structure that lies between these two well-studied morphologies with respect to the growth temperature.

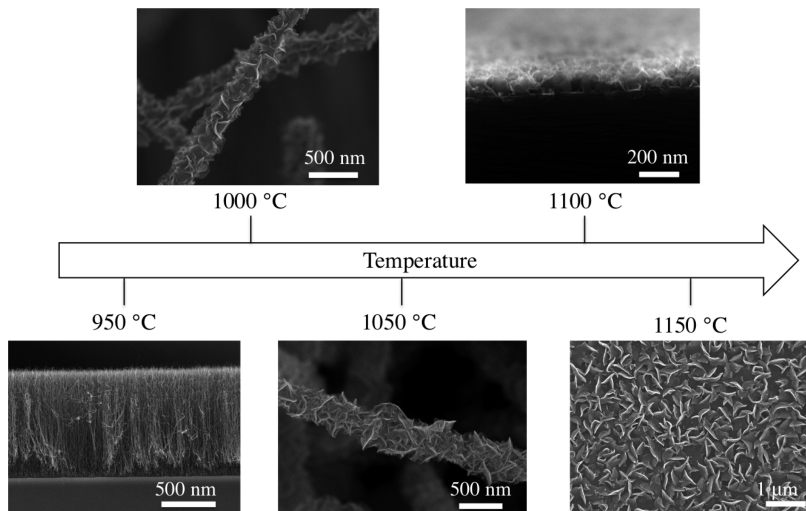


Figure 5. Morphology of the resultant films varies dramatically from the CNT structure at 950 °C, to g-CNTs at 1000 and 1050 °C, and to CNSs at 1100 °C under constant growth conditions.

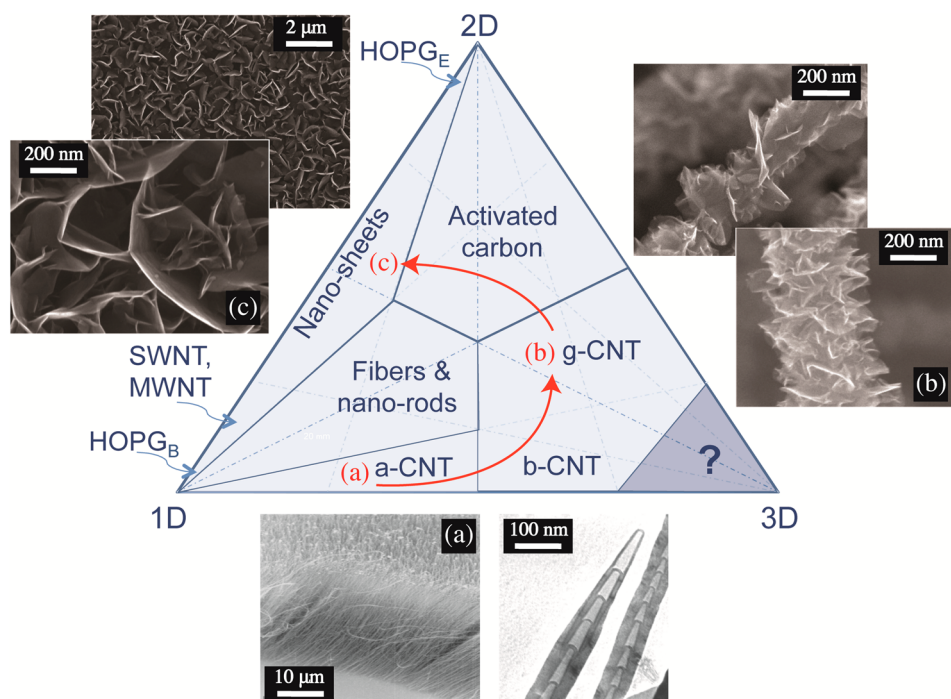


Figure 6. Electron density of graphene edges (EDGE) triangle, adapted from ref 22. The arrows indicate morphological changes that occur as process temperature is increased, from (a) aligned CNTs (a-CNT) and bamboo CNTs (b-CNT) to (b) graphenated CNTs to (c) nanosheets.

Recently, Stoner and Glass proposed a classification scheme for characterizing nanostructured carbon materials based on density of exposed graphene edges, called the electron density of graphene edges (EDGE) triangle²² (Figure 6). On the basis of studies by Randin and Yeager^{23–25} comparing the capacitance of basal- and edge-exposed highly oriented pyrolytic graphite (HOPG), graphene edges have an approximate 20-fold improvement in specific capacitance compared to planar graphene. As a result, the specific capacitance of an sp^2 -bonded carbon structure is a function of the relative concentration of edge plane exposure.^{23,26} As shown herein, varying growth temperature provides control of the edge density by enabling a transition between aligned carbon nanotubes, graphenated carbon nanotubes, and

vertically oriented graphene nanosheets. Thus, all three corners of the EDGE triangle can be traversed in a counterclockwise direction by increasing temperature, which produces structural morphologies starting from the bottom edge (a-CNTs) to the right side edge (g-CNTs) to the left edge (CNSs). In summary, this corresponds to vertical arrays of 1D structures (a-CNTs) transitioning to 3D structures (g-CNTs) and then finally to 2D structures (CNSs) with increasing temperature.

A morphology that appears to bridge the g-CNT and CNS structures was observed for structures grown in the presence of metal substrates. An experiment was designed to examine the difference in morphology between nanostructures deposited on a silicon substrate with Fe catalyst and nanostructures grown directly on a metal substrate in a microwave PECVD

environment. A Ni foil substrate without a separate catalyst layer was placed in the deposition chamber alongside a Si substrate with a 5 nm Fe catalyst layer, and nanostructures were formed at growth conditions usually associated with CNSs. The resultant film exhibited the nanosheet structure on the Ni substrate but formed a unique CNT-based hierarchical structure of ultrahigh foliate density g-CNTs, hereafter referred to as “ultra g-CNTs,” incorporating multiple secondary nucleation of graphene foliates with CNSs occupying the space between CNTs (Figure 7). The framework of the

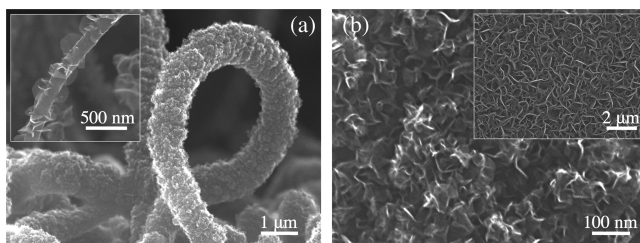


Figure 7. Ultra g-CNTs displaying multiple secondary nucleation of graphene foliates with increasing magnification from left to right. For comparison, the inset at the left represents typical g-CNTs, and the inset at the right is a CNS film grown on a silicon substrate. The framework of the structure can be seen to resemble typical g-CNTs as seen on the left, whereas the surface of the nanotube structure closely resembles vertically oriented graphene nanosheets. Nanosheets were also present at the substrate surface between the nanotube structures.

structure resembles conventional g-CNTs, whereas the surface of the nanotube structure resembles the vertically oriented CNSs. This extreme secondary nucleation resulted in an order of magnitude increase in tube diameter to $\sim 1.4 \mu\text{m}$ and may represent the region of ultrahigh edge density denoted by the question mark in Figure 6.

Temperature Effects on Specific Capacitance. A least-squares prediction profile from the DOE offers additional evidence of the relationship between temperature, morphology, and capacitance (Figure 8). The dashed lines in this plot represent 95% confidence intervals and the solid line is a least-squares curve generated from data obtained during the parametric study. It is noteworthy that while temperature is

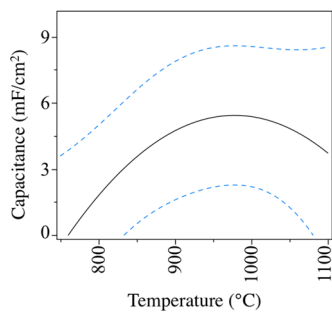


Figure 8. Standard least-squares prediction profile of capacitance (millifarads per square centimeter) as a function of deposition temperature (degrees Celsius) across all other variables within the parametric study. The solid line is a least-squares curve generated from data obtained during the parametric study, and the dashed lines in this plot represent 95% confidence intervals. The local maximum exists in the g-CNT morphological regime. Twenty-five samples were used to generate this least-squares model of capacitive response to temperature variation.

the only process parameter represented in this plot, data from variations within other process parameters are included here as well. For example, capacitance data points at a certain temperature may originate from films grown at several pretreatment times or gas ratios, which were included in the least-squares model. In this way, capacitance may be analyzed as a function of deposition temperature in the context of the entire parametric study. The local maximum in capacitance that is clear from this plot exists in the temperature regime that resulted in graphenated carbon nanotube growth during this study (925–1050 °C), indicating that the presence of few-layered graphene foliates improves the capacitive response of the material as expected from the capacitance of edges versus basal planes of sp^2 -bonded nanostructures. Figure 9 illustrates

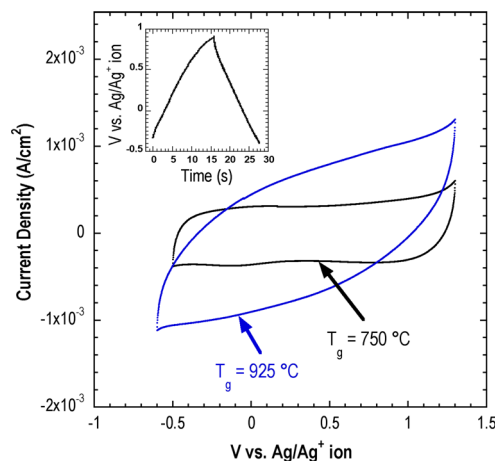


Figure 9. Cyclic voltammetry scan (scan rate, 100 mV/s) of samples with growth temperatures (T_g) of 750 and 925 °C. The sample grown at 925 °C (g-CNTs) clearly shows charge storage capacity (area under CV scan) higher than that of the 750 °C sample (CNTs). Inset: galvanostatic charge–discharging curve (at $315 \mu\text{A}/\text{cm}^2$) for sample grown at 750 °C indicating linear charging and discharging behavior.

two representative CV scans of CNTs and g-CNTs. The specific capacitance is extracted from the area under the CV curves, and it is apparent that the graphenated carbon nanotubes, grown at a higher temperature, display superior charge storage compared with that of traditional carbon nanotubes.

Foliate Formation Mechanism. As process temperature is able to control the transition between the nanotube and nanosheet structures, with g-CNTs formed at intermediate temperatures, it is of interest to examine the mechanism for the formation of this new carbon nanostructure. A stress-buckling mechanism has been previously proposed by Parker et al.,¹⁷ whereby a residual stress buildup between CNT walls with disparate growth rates causes a protrusion, which fractures and serves as a nucleation site for graphene foliates. Here we present an alternative method of foliate nucleation and growth based on a plasma etching model.

In a study analyzing the effect of pretreatment time on graphene foliate formation, a trend was observed in the uniformity of foliate coverage along the vertical direction of the CNT forest. For a growth process without any pretreatment (transitioned from thermal ramp-up in ammonia plasma directly to the deposition in ammonia/methane plasma), CNTs were produced without evidence of foliate formation. However, when a pretreatment step was introduced, foliate

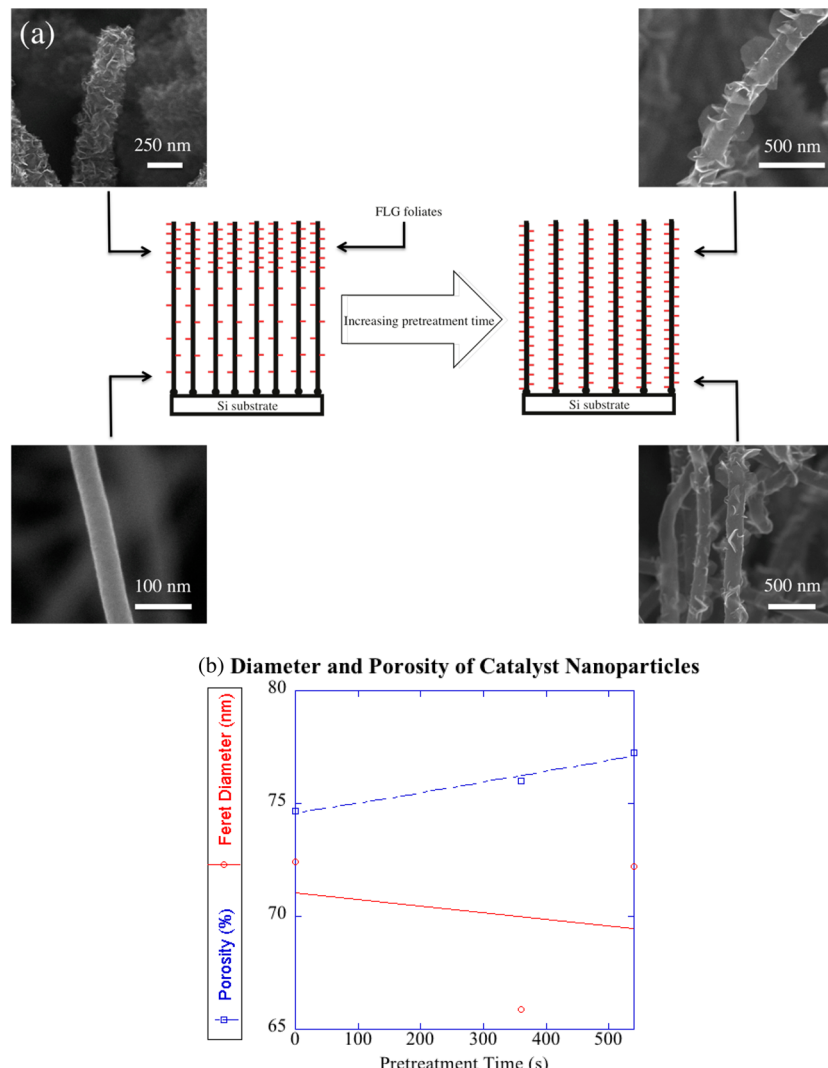


Figure 10. Effect of duration of pretreatment step. (a) When the duration of the pretreatment step is increased, the foliate density gradient is reduced. For pretreatment times less than 6 min (3 min pictured at left), graphene foliates agglomerate near the CNT tips and few are present at the CNT-substrate interface. Increasing the pretreatment time to 6 min (pictured at right) results in even foliate coverage throughout the length of the CNT forest. For pretreatment times longer than 6 min, vertical alignment becomes poor because of weakening of the crowding effect. (b) Effects of increasing pretreatment time on catalyst nanoparticles without CNT deposition.

formation occurred with higher foliate densities near the CNT tips and relatively few foliates formed near the CNT-substrate interface at low pretreatment time steps. As the pretreatment time increased, this foliate density gradient effect was diminished up to a pretreatment time of 6 min (Figure 10). At this higher pretreatment time, the foliate coverage was uniform along the length of the CNTs within the forest.

To understand the precise effect of increasing pretreatment time on the catalyst at elevated temperatures, dewetting experiments were performed by halting the g-CNT growth process just before the growth stage (prior to exposure to a carbon source gas), thus producing a two-dimensional array of catalyst nanoparticles. The pretreatment time was varied from 0 to 9 min. As seen in Figure 10b, the porosity, measured as the ratio of empty space to catalyst nanoparticle area, increased as pretreatment time increased. Additionally, the average diameter of the catalyst particles decreased slightly with increasing pretreatment time.

CNT diameters have been found to have a linear relationship with the size of the nanoparticles that catalyze their

growth;^{27–30} thus, we propose that the increase in the porosity of the CNT forest provides increased access of the reducing gas phase etchants to the entire depth of the forest (Figure 10a). As shown by Zeng et al.,¹⁰ a hydrogen plasma treatment of carbon nanotubes allowed for subsequent PECVD deposition of graphene nanosheets on the sidewalls of the CNTs, whereas without the hydrogen plasma treatment the consecutive step resulted in amorphous carbon deposition under the same growth conditions. It was proposed that some C–C bonds were replaced by C–H bonds and that some C–C bonds were broken by plasma bombardment, creating nucleation sites for the carbon nanosheets. During deposition of g-CNTs with a 50:150 sccm NH₃:CH₄ ratio, a similar mechanism of sidewall etching from NH₃ radicals and simultaneous nucleation and deposition at the defect sites could account for the formation of graphene foliates in g-CNTs in the single deposition process reported here. This mechanism is also in agreement with the observations that the graphene foliates do not form until after a critical duration of growth time is reached and that the density of foliates increases with deposition time.¹⁷

SUMMARY

The growth temperature of an MPECVD process was used to control the dimensionality and morphology of carbon nanostructures with a varying density of edges. Edge density can strongly affect charge concentration and is thus an important characteristic for such applications as supercapacitors, electrodes for neural stimulation, and electrocatalysis. An in-depth analysis using a design of experiments was performed yielding growth of CNT, g-CNT, and CNS films in the same MPECVD reactor. On the basis of statistical trends in this study, a parametric temperature series revealed that deposition temperature is the key factor in controlling nanostructure morphology, and g-CNTs emerged as a temperature-based transitional morphology between CNT and CNS structures. As predicted,²² the edge density had a significant effect on specific capacitance with the nanostructure containing greatest graphene edge density, g-CNTs, exhibiting the highest specific capacitance. Finally, an alternative g-CNT growth model to the previous stress-buckling model¹⁷ was proposed based on the plasma etching effect.

AUTHOR INFORMATION

Notes

The authors declare no competing financial interest.

ACKNOWLEDGMENTS

This work was partially supported by Grants ECCS-1344745 and DMR-1106173 from the National Science Foundation and 1R21NS070033-01A1 from the National Institutes of Health.

REFERENCES

- (1) Kroto, H. W.; Heath, J. R.; O'Brien, S. C.; Curl, R. F.; Smalley, R. E. C₆₀: Buckminsterfullerene. *Nature (London, U.K.)* **1985**, *318*, 162–163.
- (2) Iijima, S. Helical microtubules of graphitic carbon. *Nature (London, U.K.)* **1991**, *354*, 56–58.
- (3) Novoselov, K. S.; Geim, A. K.; Morozov, S.; Jiang, D.; Zhang, Y.; Dubonos, S.; Grigorieva, I.; Firsov, A. Electric field effect in atomically thin carbon films. *Science* **2004**, *306*, 666–669.
- (4) Wang, J.; Zhu, M.; Outlaw, R.; Zhao, X.; Manos, D.; Holloway, B.; Mammana, V. Free-standing subnanometer graphite sheets. *Appl. Phys. Lett.* **2004**, *85*, 1265–1267.
- (5) Wu, Y.; Yu, T.; Shen, Z. Two-dimensional carbon nanostructures: Fundamental properties, synthesis, characterization, and potential applications. *J. Appl. Phys.* **2010**, *108*, 071301.
- (6) Pumera, M.; Ambrosi, A.; Bonanni, A.; Chng, E. L. K.; Poh, H. L. Graphene for electrochemical sensing and biosensing. *TrAC, Trends Anal. Chem.* **2010**, *29*, 954–965.
- (7) Wei, D.; Liu, Y. Controllable synthesis of graphene and its applications. *Adv. Mater. (Weinheim, Ger.)* **2010**, *22*, 3225–3241.
- (8) Trasobares, S.; Ewels, C. P.; Birrell, J.; Stephan, O.; Wei, B. Q.; Carlisle, J. A.; Miller, D.; Kebinski, P.; Ajayan, P. M. Carbon nanotubes with graphitic wings. *Adv. Mater. (Weinheim, Ger.)* **2004**, *16*, 610–613.
- (9) Yu, K.; Lu, G.; Bo, Z.; Mao, S.; Chen, J. Carbon nanotube with chemically bonded graphene leaves for electronic and optoelectronic applications. *J. Phys. Chem. Lett.* **2011**, *2*, 1556–1562.
- (10) Zeng, L.; Lei, D.; Wang, W.; Liang, J.; Wang, Z.; Yao, N.; Zhang, B. Preparation of carbon nanosheets deposited on carbon nanotubes by microwave plasma-enhanced chemical vapor deposition method. *Appl. Surf. Sci.* **2008**, *254*, 1700–1704.
- (11) Fan, Z.; Yan, J.; Zhi, L.; Zhang, Q.; Wei, T.; Feng, J.; Zhang, M.; Qian, W.; Wei, F. A Three-Dimensional Carbon Nanotube/Graphene Sandwich and Its Application as Electrode in Supercapacitors. *Adv. Mater. (Weinheim, Ger.)* **2010**, *22*, 3723–3728.
- (12) Yu, D.; Dai, L. Self-assembled graphene/carbon nanotube hybrid films for supercapacitors. *J. Phys. Chem. Lett.* **2010**, *1*, 467–470.
- (13) Yoo, E.; Kim, J.; Hosono, E.; Zhou, H.-s.; Kudo, T.; Honma, I. Large reversible Li storage of graphene nanosheet families for use in rechargeable lithium ion batteries. *Nano Lett.* **2008**, *8*, 2277–2282.
- (14) Tung, V. C.; Chen, L.-M.; Allen, M. J.; Wassei, J. K.; Nelson, K.; Kaner, R. B.; Yang, Y. Low-temperature solution processing of graphene–carbon nanotube hybrid materials for high-performance transparent conductors. *Nano Lett.* **2009**, *9*, 1949–1955.
- (15) Stoner, B. R.; Raut, A. S.; Brown, B.; Parker, C. B.; Glass, J. T. Graphenated carbon nanotubes for enhanced electrochemical double layer capacitor performance. *Appl. Phys. Lett.* **2011**, *99*, 183104.
- (16) Liyanage, L. S.; Cott, D. J.; Delabie, A.; Van Elshocht, S.; Bao, Z.; Wong, H. P. Atomic layer deposition of high-k dielectrics on single-walled carbon nanotubes: A Raman study. *Nanotechnology* **2013**, *24*, 245703.
- (17) Parker, C. B.; Raut, A. S.; Brown, B.; Stoner, B. R.; Glass, J. T. Three-dimensional arrays of graphenated carbon nanotubes. *J. Mater. Res.* **2012**, *27*, 1046–1053.
- (18) Cui, H.; Zhou, O.; Stoner, B. R. Deposition of aligned bamboo-like carbon nanotubes via microwave plasma enhanced chemical vapor deposition. *J. Appl. Phys.* **2000**, *88*, 6072–6074.
- (19) Wang, J.; Zhu, M.; Outlaw, R. A.; Zhao, X.; Manos, D. M.; Holloway, B. C. Synthesis of carbon nanosheets by inductively coupled radio-frequency plasma enhanced chemical vapor deposition. *Carbon* **2004**, *42*, 2867–2872.
- (20) Raut, A. S.; Parker, C. B.; Glass, J. T. A method to obtain a Ragone plot for evaluation of carbon nanotube supercapacitor electrodes. *J. Mater. Res.* **2010**, *25*, 1500–1506.
- (21) Conway, B. E. *Electrochemical Supercapacitors: Scientific Fundamentals and Technological Applications*; Kluwer Academic/Plenum Publishers: New York, NY, 1999.
- (22) Stoner, B. R.; Glass, J. T. Carbon nanostructures: A morphological classification for charge density optimization. *Diamond Relat. Mater.* **2012**, *23*, 130–134.
- (23) Randin, J.-P.; Yeager, E. *Differential Capacitance Study of Stress-Annealed Pyrolytic Graphite Electrodes*; Office of Naval Research: Arlington, VA, 1970.
- (24) Randin, J.-P.; Yeager, E. Differential capacitance study on the basal plane of stress-annealed pyrolytic graphite. *J. Electroanal. Chem. Interfacial Electrochem.* **1972**, *36*, 257–276.
- (25) Randin, J.-P.; Yeager, E. Differential capacitance study on the edge orientation of pyrolytic graphite and glassy carbon electrodes. *J. Electroanal. Chem. Interfacial Electrochem.* **1975**, *58*, 313–322.
- (26) Qu, D. Studies of the activated carbons used in double-layer supercapacitors. *J. Power Sources* **2002**, *109*, 403–411.
- (27) Huang, Z.; Wang, D.; Wen, J.; Sennett, M.; Gibson, H.; Ren, Z. Effect of nickel, iron and cobalt on growth of aligned carbon nanotubes. *Appl. Phys. A: Mater. Sci. Process.* **2002**, *74*, 387–391.
- (28) Wang, Y.; Gupta, S.; Nemanich, R. Role of thin Fe catalyst in the synthesis of double- and single-wall carbon nanotubes via microwave chemical vapor deposition. *Appl. Phys. Lett.* **2004**, *85*, 2601–2603.
- (29) Wang, Y.; Gupta, S.; Nemanich, R.; Liu, Z.; Qin, L. Hollow to bamboo-like internal structure transition observed in carbon nanotube films. *J. Appl. Phys.* **2005**, *98*, 014312.
- (30) Yamada, T.; Namai, T.; Hata, K.; Futaba, D. N.; Mizuno, K.; Fan, J.; Yudasaka, M.; Yumura, M.; Iijima, S. Size-selective growth of double-walled carbon nanotube forests from engineered iron catalysts. *Nat. Nanotechnol.* **2006**, *1*, 131–136.